ELSEVIER

Journal of Photochemistry and Photobiology A: Chemistry 144 (2001) 205–213

Journal of Photochemistry and Photobiology A:Chemistry

www.elsevier.com/locate/jphotochem

Mechanism of photocatalytic oxidation of 3,4-dichlorophenol on TiO_2 semiconductor surfaces

Anna-Karin Axelsson [a], Lawrence J. Dunne [a,b,*]

[a] *School of Applied Science, South Bank University, London SE1 0AA, UK*

[b] *School of Chemistry, Physics and Environmental Science, University of Sussex, Falmer, Brighton BN1 9QJ, UK*

Received 20 March 2001; accepted 3 August 2001

Abstract

In this paper, the results of a detailed study of the kinetics of photocatalytic oxidation of 3,4-dichlorophenol at various concentrations in oxygenated solutions on TiO_2 are presented. Electron–hole recombination is often suggested to be decreased by increasing the molecular oxygen concentration; but our study indicates that this is not the primary rate enhancing property of the dissolved oxygen. It is argued here that a hydroxyl radical is ejected from the catalyst surface by photo-excitation onto a repulsive excited electronic state leading to a translationally hot $OH(^2\pi)$ radical. In the presence of molecular oxygen, a simple hydroxyl addition to the dichlorophenol occurs. In the absence of an adsorbed oxygen molecule, the electron transfer to the aromatic ring from a Ti^{3+} site causes partial dechlorination of the dichlorophenol. Subsequently, hydroxyl radical addition to the aromatic ring may occur. Hence, we find that dissolved molecular oxygen has two important roles in the photo-catalytic oxidation of 3,4-dichlorophenol on the semiconducting TiO_2 surfaces. One of these is as a H-atom acceptor required in direct hydroxyl radical addition to the phenyl ring while the other is as an electron transfer inhibitor when adsorbed at defective Ti^{3+} sites. A theoretical model of the kinetics is proposed which is able to account semi-quantitatively for the overall features of the reaction state space. Significantly, monitoring of the intermediate species produced by these two routes shows that the relative yields can be inverted by changing the dissolved oxygen concentration which significantly is accord with the theoretical predictions.

Keywords: 3,4-Dichlorophenol; Photo-catalysis; TiO_2; Oxygen

1. Introduction

Toxic chloroaromatic compounds may be removed from the effluents by catalytic photo-oxidation [1,2] but the mechanism of such light induced degradation is still unresolved [7–13,15]. In this paper, the results of a detailed study of the kinetics of photo-oxidation of 3,4-dichlorophenol at various concentrations in the oxygenated solution on TiO_2 and TiO_2/SnO_2 are presented and a kinetic model of the system proposed. Illumination of photo-catalytic semiconducting TiO_2 based surfaces at energies above the band gap produces charge carriers (electron and holes) [8,9] which are the primary cause of the photochemical events. Electron–hole recombination competes with photochemical oxidation processes and retardation of this may increase the desired yield. Such electron–hole recombination is often suggested to be decreased by increasing the molecular oxygen concentration, but our study indicates that this is not the primary rate enhancing property of the dissolved oxygen. In our elucidation of the mechanism of photo-catalytic oxidation of 3,4-dichlorophenol on the catalyst surfaces, we have been guided by product formation in flash photolysis [3] of chlorophenols in water, where $OH(^2\pi)$ radicals and solvated electrons may also be present. With chlorophenol, the dominant reaction with $OH(^2\pi)$ radicals is addition to the aromatic ring without dechlorination is shown below (where R = phenyl–OH and $OH^\bullet = OH(^2\pi)$)

$$RCl + OH^\bullet \rightarrow [ROHCl]^\bullet$$

Removal of a hydrogen atom from $[ROHCl]^\bullet$ requires some other radical or an oxidising agent [4]. In oxygenated solutions, the most likely species to achieve this hydrogen accepting role is molecular oxygen as shown as follows:

$$[ROHCl]^\bullet + O_2 \rightarrow ROHCl + HO_2^\bullet$$

where the above step is rate determining.

The free electrons generated in flash photolysis reduce the chlorophenols directly [3].

$$RCl + e^- \rightarrow R^\bullet + Cl^-$$

* Corresponding author. Tel.: +44-207-815-7944; fax: +44-207-815-7999.
E-mail address: dunnel@vax.sbu.ac.uk (L.J. Dunne).

1010-6030/01/$ – see front matter
PII: S1010-6030(01)00536-6

Addition of an OH radical then leads to

$$R^{\bullet} + OH^{\bullet} \rightarrow ROH$$

These reaction schemes shown above seem to occur in the photo-catalytic oxidation of 3,4-dichlorophenol on TiO_2. Thus, a major role for molecular oxygen in photo-catalytic oxidation of chlorophenols appears to be as a hydrogen atom acceptor following hydroxyl radical addition to an aromatic ring [4].

Adsorbed water on the surface of TiO_2 appears to photodissociate generating an OH radical. A process with similar features is the photo-dissociation of water in the gas phase [5,6]. In the latter photo-dissociation, an $OH(^2\pi)$ radical is ejected in a hot ro-vibrational and translational state from the parent water molecule, by surface crossing onto a repulsive π-surface associated with a conical intersection in linear configurations of the molecule [5]. Several authors [7–11] have suggested that the OH radical generated by illumination of the catalyst surface plays a dominant role in the photo-catalytic oxidation process. Turchi and Ollis [7] proposed that the generated OH radical might diffuse into the solid–liquid interfacial region. A further important study by Mills and Wang [12] on photo-catalytic oxidation of 4-chlorophenol showed that the formation of the OH radical and the dissolved oxygen level have an important influence on the rate of reaction. Related work by Serpone et al. [13] have demonstrated the dechlorination of dichlorophenols at oxygen free TiO_2–water interfaces in the presence of hole scavengers. Tang and Huang established that hydroxyl radical attack the unoccupied sites of the chloroaromatic ring and that chlorine atom will be released from the chlorinated aliphatic intermediates instead of the aromatic ring when Fenton's reagent was used as a source of OH radicals [14]. Other recent kinetic studies by Zoulalian and co-workers [15] of the photo-oxidation of 2-chlorophenol and 4-chlorophenol by TiO_2 have suggested the importance of the adsorption of O_2 on the defective Ti^{3+} sites. Here, we present the outcome of an experimental study and theoretical analysis of the photochemical oxidation of 3,4-dichlorophenol on TiO_2 and TiO_2/SnO_2 at a range of concentrations and dissolved oxygen levels. Coupling of two semiconductors, possessing different redox energy levels for their corresponding conduction band and reduction band, provides another approach to achieve a more efficient charge separation and increase the lifetime of the charge carriers.

A model is proposed which accounts successfully for the essential features of the photochemical oxidation process and which is a hybrid of the suggestions for the mechanism put forward by the above workers [1,3,7–13] and reviewed there. It is argued here that the hydroxyl radical is ejected from the catalyst surface by photo-excitation onto a repulsive excited electronic state leading to a translationally hot $OH(^2\pi)$ radical, which relates to the Turchi and Ollis proposal [7] for diffusion of the radical into the interfacial region. In the presence of molecular oxygen, simple hydroxyl addition to the dichlorophenol occurs. In the absence of an adsorbed oxygen molecule, the electron transfer to the aromatic ring from a Ti^{3+} site causes partial dechlorination of the dichlorophenol. Subsequently, hydroxyl radical addition to the aromatic ring may occur. Hence, we find that dissolved molecular oxygen has two important roles in the photo-catalytic oxidation of 3,4-dichlorophenol on the semiconducting TiO_2 surfaces. One of these is as a H-atom acceptor required in the direct hydroxyl radical addition to the phenyl ring, while the other is as an electron transfer inhibitor when adsorbed at defective Ti^{3+} sites. A theoretical model of the kinetics suggests that the former process may increase in rate while the latter process should be inhibited by molecular oxygen and such an effect is observed experimentally. Significantly, monitoring of the intermediate species produced by these two routes shows that the relative yields can be inverted by changing the dissolved oxygen concentration and as such is a striking feature which is in accordance with the theoretical predictions. Such an inversion is easily observed in this system because of the fortuitous balance of the kinetic parameters for 3,4-dichlorophenol enabling the cross-over of rates with increasing dissolved oxygen concentration to be straightforwardly monitored.

Ti and O have a rich mixed valence chemistry and a defective TiO_2 surface will contain Ti^{4+}, Ti^{3+}, O^- and O^{2-} ions [16]. These are associated with the surface random potential and deep electron and hole traps. Molecular oxygen (O_2) preferentially adsorbs at Ti^{3+} ions [12]. Organic species adsorb preferentially at Ti^{4+} sites. At an aqueous interface, these sites will be hydrated giving bound OH^- ions anatase as shown by infrared evidence [17].

2. Experimental

2.1. Catalyst preparation and characterisation

Immobilised catalyst plates were prepared using equimolar amount of TiO_2 (Degussa P25) and SnO_2 (Alfa 99%) in a slurry which was ultra-sonicated for 20 min and coated onto alumina sheets.

Scanning electron micrographs (Hitachi S800) were taken and a typical example in Fig. 1 appears smooth and dense to the naked eye, shows a clear evidence of high porosity. The smaller particles (size of approximately 50–60 nm are TiO_2) and slightly bigger clusters (size 120–150 nm) are SnO_2. In the following discussion, the results presented are virtually identical for both types of catalyst plates with the SnO_2 coupled plates being marginally more active.

Adsorption spectra of the plates were obtained by using a dual beam spectrophotometer (Perkin-Elmer Lambda 20) with a background adjusted against a white zero sample (Lab Sphere ID: USRS-99-010).

The absorption spectra shown in Fig. 2, shows a band edge at 395 nm (3.05 eV) for TiO_2 (P25) and SnO_2 at 365 nm (3.29 eV). Hence, a "blacklight" fluorescence lamp and with

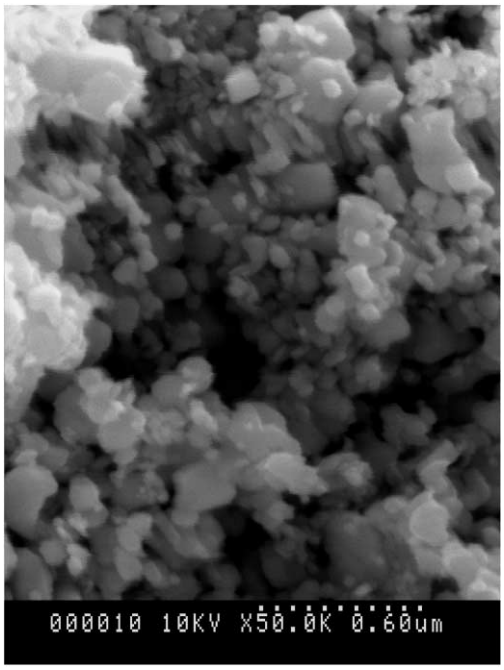

Fig. 1. SEM image of a packed SnO_2/TiO_2 powder surface.

an irradiation output between 360 and 370 nm will primarily excite the TiO_2.

2.2. Photocatalytic reactor

The reactor, connected to a replacement pump via an inlet and outlet, consists of a highly polished stainless steel box that houses the immobilised catalyst plate. The reactor chamber was thermostated to 18°C by a cooling jacket. A typical flow rate was up to 260 ml/min and the recycled batch was 270 ml. An important feature of catalytic heterogeneous processes is the possible control of the reaction rate by either diffusion or of the intrinsic rate on the surface. Experiments were performed at several flowrates but no significant effect on photochemical kinetics could be observed. This is consistent with the small mass-transfer effect expected at low irradiation levels.

As a light source a "blacklight" fluorescence lamp (Philips 15 W) maximum output at 365 nm was used. The light tube was placed 50 mm from the catalyst surface, inside the reactor. The photon output from the lamp has been estimated using data given by the manufacturer (Philips Eindhoven) to be approximately 10^{-8} Einstein/cm^2 which is low enough for the rate to be less than the mass-transfer diffusion controlled limit [18].

To examine the effect of dissolved O_2 on the 3,4-dichlorophenol degradation, either N_2 or O_2 gas was bubbled through the reactor solution throughout a run, thereby, varying the dissolved oxygen level between 2.0 and 30.0 ppm.

2.3. Analysis

All reactor runs were carried out for several hours and samples were taken regularly and analysed chromatographically (HPLC and GC–MS) and spectrophotometrically (Perkin-Elmer Lamba 20). A simultaneous pH reading was carried out to monitor the HCl production.

HPLC instrumentation (Waters), with Millenium 2010 Chromatography Manager software together with a non-polar column (Wakosil II^{TM} 5C18AR 250 mm × 4.5 mm) and detector (Waters 996 photodiode array detector) was set

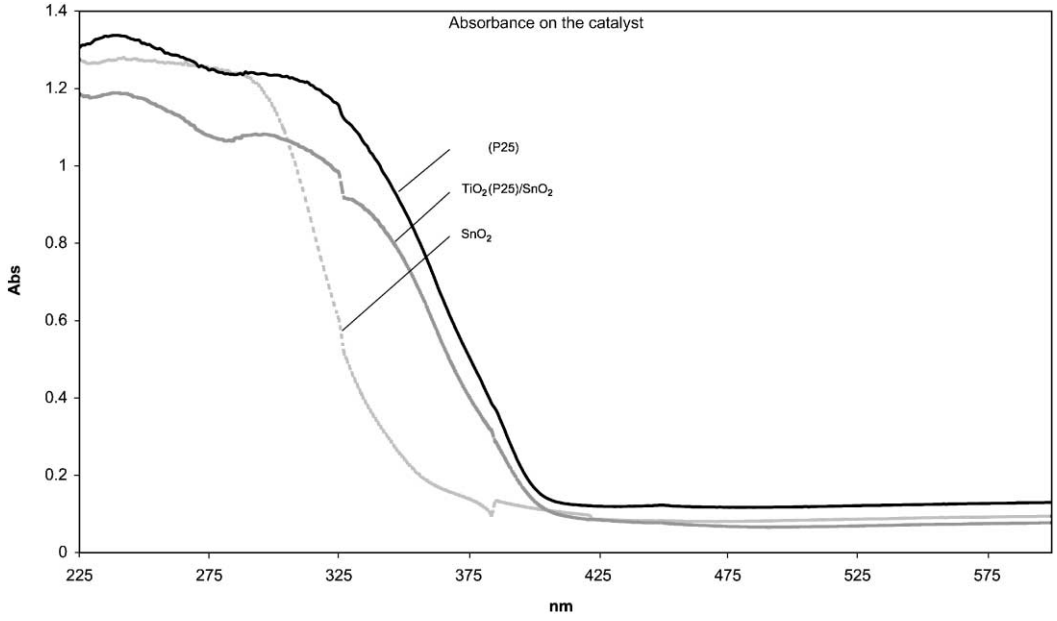

Fig. 2. Absorption spectra of annealed TiO_2 (P25)/SnO_2, TiO_2(P25) and SnO_2.

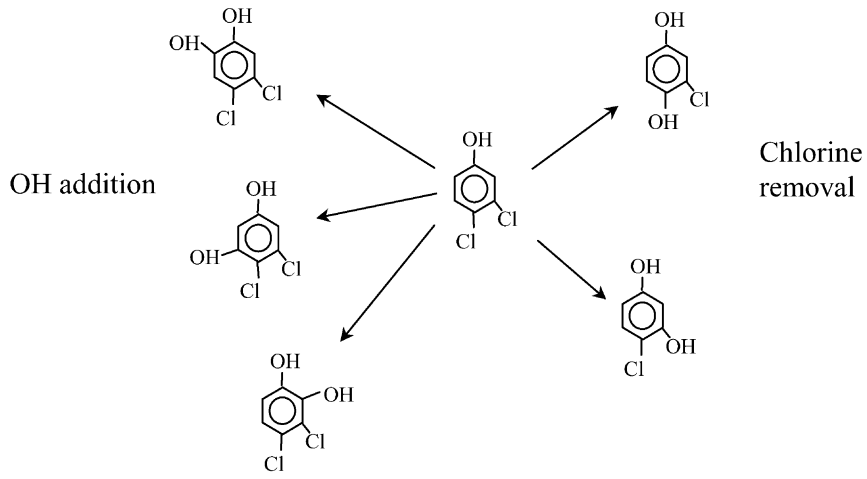

Fig. 3. Suggested primary intermediate formation from photo-catalytic oxidation of 3,4-dichlorophenol.

to 273 nm. GC–MS instrumentation set-up was GC–MS (Fison 8065) with Autolab software and NIST library, column (100 m DBI ∅ 2.3 mm, film thickness 0.5 μm) and detector (Fison MD800). Oxygen concentration was measured by an oxygen membrane electrode.

3. Experimental results

By comparing GC–MS and HPLC data together with UV–VIS spectra the following dominant primary intermediates are shown below were observed.

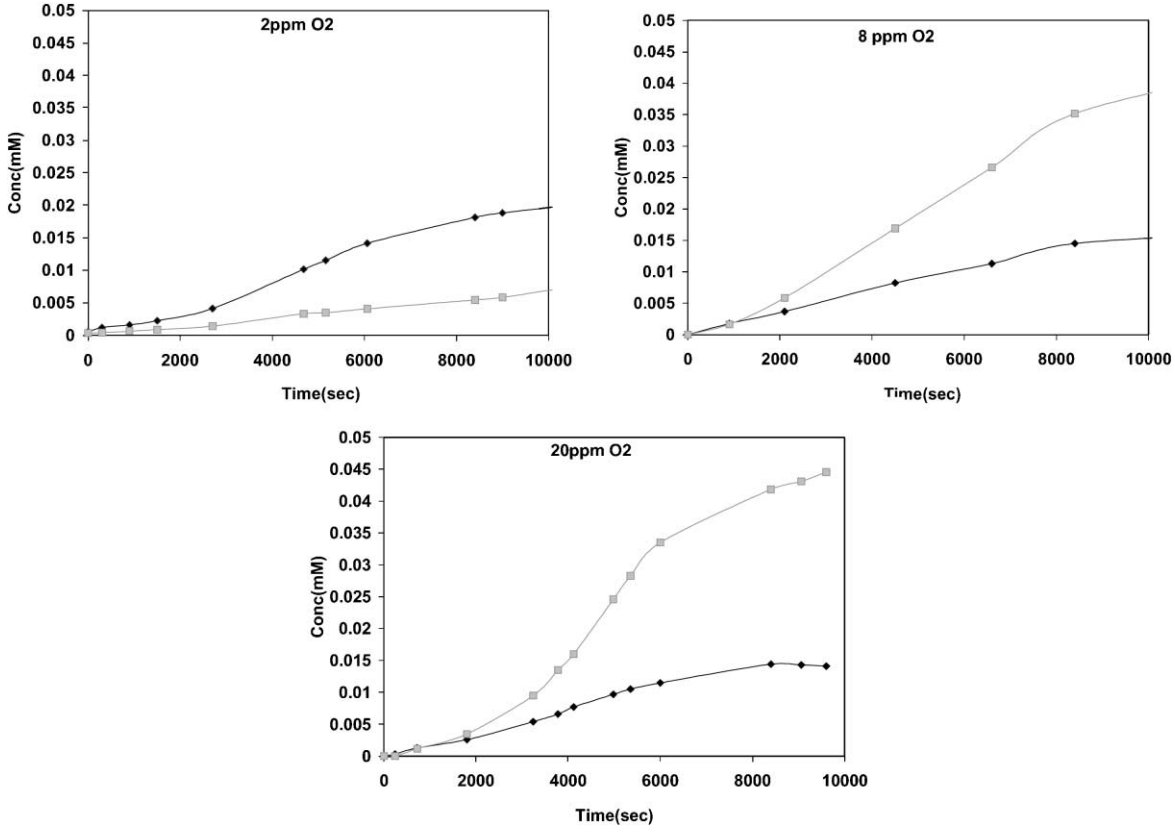

Fig. 4. Yield of OH addition (□) and chlorine removal routes (◆) formed in photo-catalytic oxidation of 1 mmol 3,4-dichlorophenol at low, ambient and high oxygen level.

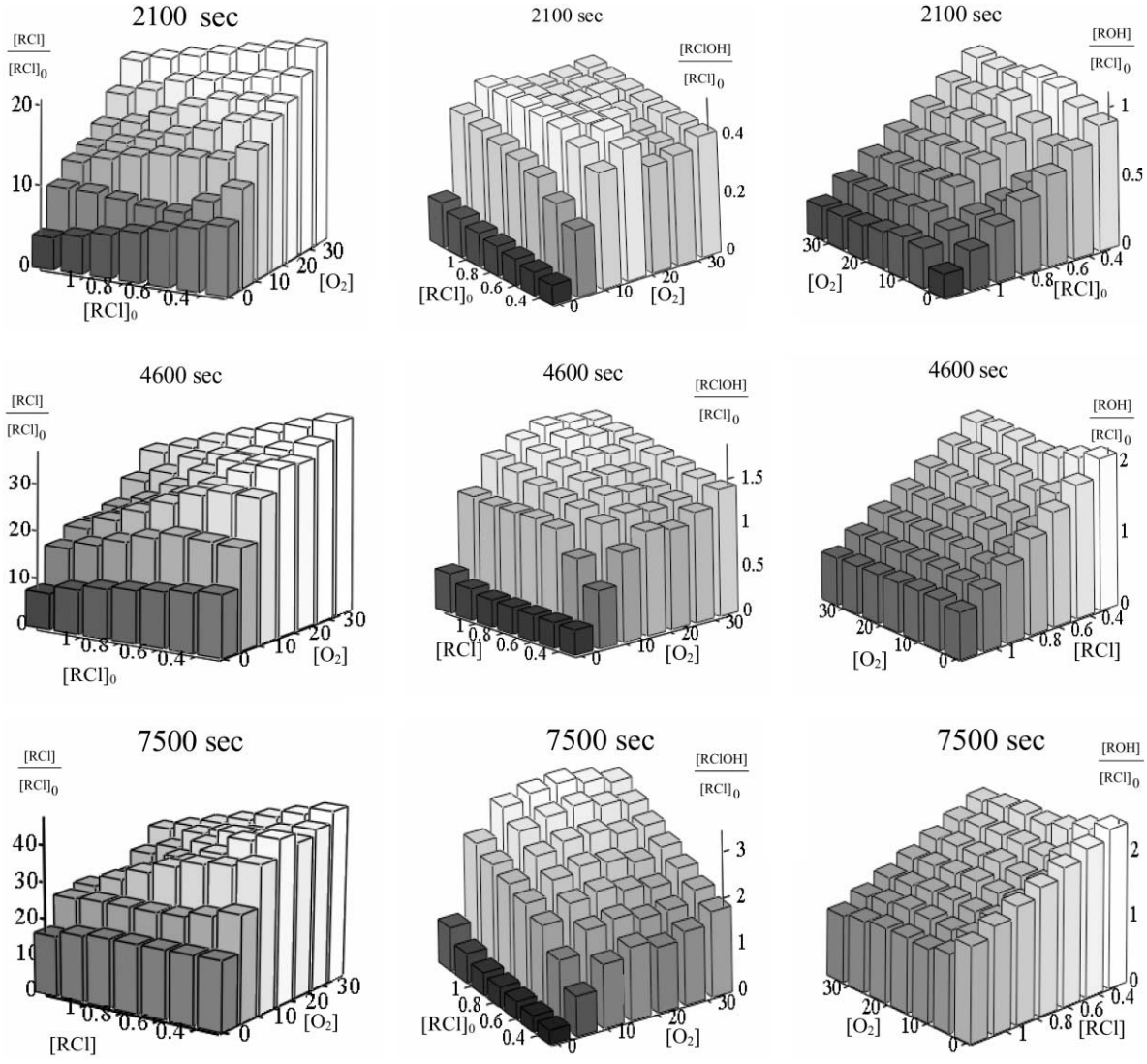

Fig. 5. 3D view showing the yield of 3,4-dichlorophenol disappearance as a function of initial concentration and oxygen level at 2100, 4600 and 7600 s reaction times, respectively, to the left and yield of OH addition in the middle and Cl removal to the right.

The section to the left, involves chlorine removal from the 3,4-dichlorophenol, while the section to the right involves an OH radical addition to the ring.

The main products detected were classified as to whether simple OH addition had occurred or chlorine removal followed by hydroxylation had occurred. Typically, each reactor run was repeated four times with a fresh catalyst. Runs were undertaken at various oxygen levels and initial concentrations of 3,4-dichlorophenol. Fig. 3 shows the two intermediate formations from the photo-catalytic oxidation of 3,4-dichlorophenol. It can be seen in Fig. 4 how the yield of the two types of intermediate (shown in Fig. 3) inverts with the chlorine removal least effective in high oxygen and OH addition least effective in low oxygen.

The experimental yields, expressed as $[RCl]/RCl]_0$ for the 3,4-chlorophenol, $[RClOH]/[RCl]_0$ for the OH addition route and $[ROH]/[RCl]_0$ for the dechlorination route, are shown in Fig. 5 for various initial parent compound $[RCl]_0$ and oxygen concentrations $[O_2]$ at a selection of reaction times (2100, 4600 and 7500 s, respectively).

It can be seen that the yield ($[RCl]/[RCl]_0$) is higher for low initial parent compound $[RCl]_0$ concentrations and high oxygen concentrations $[O_2]$. Most interestingly, the yield of the intermediates for the OH addition and dechlorination routes cross over with dissolved oxygen concentration (see Fig. 4) with the highest yield for the dechlorination route at the lowest oxygen level and at the highest oxygen level for the simple OH addition route.

4. Surface crossing and photo-ejection of OH($^2\pi$) radicals from TiO_2

It is widely assumed that the TiO_2 surface is hydroxylated when in contact with water [7,9,19]. Although, TiO_2 can be largely regarded as having the formula Ti^{4+} O_2^{2-}.

Degussa P25 (which is predominately anatase) is a mixed valence compound some of the surface sites must be formally regarded as Ti^{3+} and O^- ions particularly at surface defect sites, giving rise to impurity bands in the material. If the defect concentration is, high it is likely that these defects will pin the Fermi level to a position mid-way between the valence and conduction bands as in amorphous materials [20,21]. It is widely believed that such Ti^{3+} sites can be partially oxidised by binding molecular O_2 and that organic substrates bind to surface $Ti^{4+}OH^-$ groups [15].

The simplest model of the photochemisty of water on the surface of anatase can be derived from the studies [17] which show dissociated water molecules at low coverage. We may write the removal of an OH fragment from a dissociated water molecule adsorbed on a TiO_2 fragment in anatase (generally represented as $(TiO_2)_nH)^+$ OH^-) as following the scheme:

$$((TiO_2)_nH) + OH^- \rightarrow ((TiO_2)_nH))^+ \cdots OH^- \quad (a)$$

$$((TiO_2)_nH) + OH^- \rightarrow ((TiO_2)_nH) \cdots OH(^2\pi) \quad (b)$$

At the dissociation limit, channel (a) is endothermic by I–A, where I is the ionisation potential of the $((TiO_2)_nH)$ cluster (estimated to be about 5 eV from the density functional calculations on hydrated TiO_2 [19]) and A the electron affinity of $OH(^2\pi)$ which is known to be about 1.8 eV [22]. The numerical value of I–$A = 3.2$ eV should be roughly equal to the charge transfer gap in hydrated anatase which we estimate spectroscopically to be 3.07 eV from the absorption edge in a surface reflectance spectrum. At short range, this energy cost will be offset by the electrostatic energy change at the charged centre from which the OH^- ion has been removed. Added to this energy is a short range repulsive interaction of the form $U_{rep}(R) = a \cdot \exp(b(R_e - R))$, where R_e is taken as 1.9 Å which is the equilibrium TiO bond length [16] and $a = 2.9$ eV and $b = 4.0$/Å. The two adiabatic potential energy curves [23] are shown in Fig. 6.

The point of interest is that an $OH(^2\pi)$ fragment excited onto the upper state will be ejected from the surface following the well-known harpoon mechanism [24]. Illumination will cause the ejection of translationally hot $OH(^2\pi)$ radicals from the hydrated TiO_2 surface. The excess kinetic energy is of the order 0–1 eV. The hot OH radical may undergo reactive collision with an organic species in the interfacial region. The electron released from the OH^- ion can be injected in the Ti^{3+} impurity band of the TiO_2 and by tunnelling across the interfacial region at an oxygen free Ti^{3+} site, can directly reduce the organochlorine compounds. Based on these assumptions, we have formulated a kinetic model presented in the following section.

5. Kinetic model

We consider a surface containing two types of active sites, i.e. Ti^{3+} and Ti^{4+}. The former site may be vacant or occupied by an oxygen molecule, while the latter may be hydrated and bind the organochlorine molecules. The rate of equilibration of the surface and bulk concentrations is assumed to be faster than any of the surface reactions, which is justified for the low photon flux used in our experiment and referred to earlier.

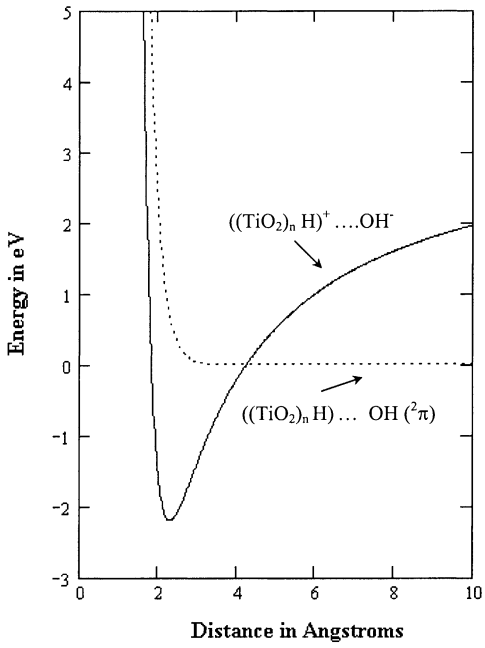

Fig. 6. Suggested adiabatic potential energy curves for removal of an OH fragment from a hydrated anatase surface. The higher energy curve on the left corresponds to OH^- whole the lower curve to OH.

Light is assumed to generate OH radicals at Ti^{4+} sites and collision with aromatic organochlorine (RCl) compounds is expected to yield the intermediate $[ROHCl]^\bullet$.

$$RCl + OH^\bullet \rightarrow [ROHCl]^\bullet$$

Molecular oxygen bound at the neighbouring Ti^{3+} site may then remove a hydrogen atom from $[ROHCl]^\bullet$ as follows:

$$[ROHCl]^\bullet + O_2 \rightarrow ROHCl + HO_2^\bullet$$

The $HO_2^\bullet$ radical generated may react with the H atom remaining from the photo-dissociation of surface bound water to give

$$HO_2^\bullet + H^\bullet \rightarrow H_2O_2$$

In the absence of O_2 the alternative reaction

$$[ROHCl]^\bullet + H^\bullet \rightarrow ROHCl + H_2$$

generates molecular hydrogen and this is observed experimentally in the photo-oxidation on TiO_2 [10]

Reaction of organochlorine compounds with photogenerated electrons available at the Ti^{3+} site leads to chlorine removal.

$$RCl + e^- \rightarrow R^\bullet + Cl^-$$

Addition of an OH radical then leads to

$$R^{\bullet} + OH^{\bullet} \rightarrow ROH$$

The released Cl^- anion picks up the surface bound proton remaining after the release of the free electron from the TiO_2 surface to give $Cl^- + H^+ \rightarrow HCl$. The generation of HCl was observed experimentally by monitoring the pH changes. If O_2 molecules block the Ti^{3+} site, the above reaction will not proceed. We assume that the fraction, Θ of hydrated Ti^{4+} sites occupied by organic species $i = 1, 2, 3$ is given by

$$\Theta_i = \frac{K_{ads}[c]_i}{1 + K_{ads}\sum_i [c]_i}$$

where, for simplicity, each compound has the same Langmuir adsorption constant K_{ads}. Oxygen adsorption on the Ti^{3+} sites also obeys Langmuir adsorption isotherm, so that the fraction of these sites occupied by an oxygen molecule is given by

$$\Theta_{oxygen} = \frac{K_{ox}[O]}{1 + K_{ox}[O]}$$

Therefore, the fraction of Ti^{3+} sites available for direct reduction of the chloroaromatic species is given by

$$1 - \frac{K_{ox}[O]}{1 + K_{ox}[O]} = 1 - K'[O]$$

The classification of the above findings is shown in the kinetic model scheme presented in Fig. 7; while the outcome of these findings is shown in Fig. 8. The compounds in box (b) are chlororesorcinol and chlorohydroxyquinone, where 3,4-dichlorophenol has lost a chlorine atom, which subsequently has been replaced by a hydroxyl radical. The compounds in box (c) are dichlorobenzodiols where 3,4-dichlorophenol has undergone direct hydrogen substitution by a hydroxyl radical. These groups are subsequently forming further aliphatic species and finally the end products, CO_2, H_2O and HCl. The compounds in the boxes (d)–(g) are a combination of formed aliphates and highly hydroxylated compounds where accurate concentration measurements proved difficult.

The rate of loss of the parent compound (neglecting the adsorption on the catalyst, etc.) is given by the sum of the rates for hydroxyl radical addition and the dichlorination channels. The rate for direct hydroxyl radical addition (which requires the presence of an oxygen molecule on a Ti^{3+} site neighbouring the organic species on the hydrated Ti^{4+} site) is proportional to

$$\frac{[OH]K_{ads}[a]K'[O]}{1 + K_{ads}[a] + K_{ads}[b] + K_{ads}[c]}$$

The rate of dichlorination by electron transfer from an oxygen free Ti^{3+} site is proportional to

$$\frac{[OH]K_{ads}[a](1 - K'[O])}{1 + K_{ads}[a] + K_{ads}[b] + K_{ads}[c]}$$

In the steady state, the rate constants of proportionality and the OH concentration can be expressed as single effective pseudo rate constants (k_{ab} and k_{ac}, respectively).

Based on these assumptions, the kinetic equations for the entire reaction scheme is given by

$$\frac{d[a]}{dt} = \frac{-K_{ads}[a]k_{ac}K'[O] + K_{ads}k_{ab}[a](1 - K'[O])}{1 + K_{ads}[a] + K_{ads}[b] + K_{ads}[c]}$$

$$\frac{d[b]}{dt} = \frac{K_{ads}k_{ab}[a](1 - K'[O]) - K_{ads}k_{bd}[b]K'[O] - K_{ads}k_{be}[b](1 - K'[O])}{1 + K_{ads}[a] + K_{ads}[b] + K_{ads}[c]}$$

$$\frac{d[c]}{dt} = \frac{K_{ads}k_{ac}[a]K'[O] + K_{ads}k_{cf}[c](1 - K'[O]) - K_{ads}k_{cg}[c]K'[O])}{1 + K_{ads}[a] + K_{ads}[b] + K_{ads}[c]}$$

These equations were solved numerically for plausible values of the rate constants and other parameters given in Fig. 5 caption. The model predicts a striking cross over in the rates of the routes with increasing oxygen concentration.

The model parameters, which gave a fit to the overall trends were $k_{ab} = 0.9 \times 10^{-8}$ mmol/s, $k_{bd} = 1 \times 10^{-10}$ mmol/s, $k_{be} = 1 \times 10^{-10}$ mmol/s, $k_{ac} = 0.9 \times 10^{-7}$ mmol/s, $k_{cf} = 1.5 \times 10^{-6}$ mmol/s, $k_{cg} = 1.5 \times 10^{-6}$ mmol/s. Plausible values for K_{ox} is 9600/mol [15] and $K_{ads} = 3600$/mol [15].

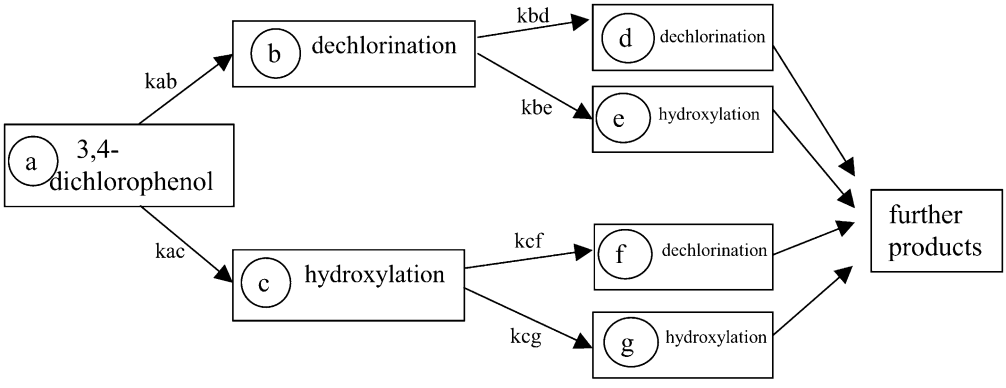

Fig. 7. Reaction scheme used in kinetic modelling of 3,4-dichlorophenol.

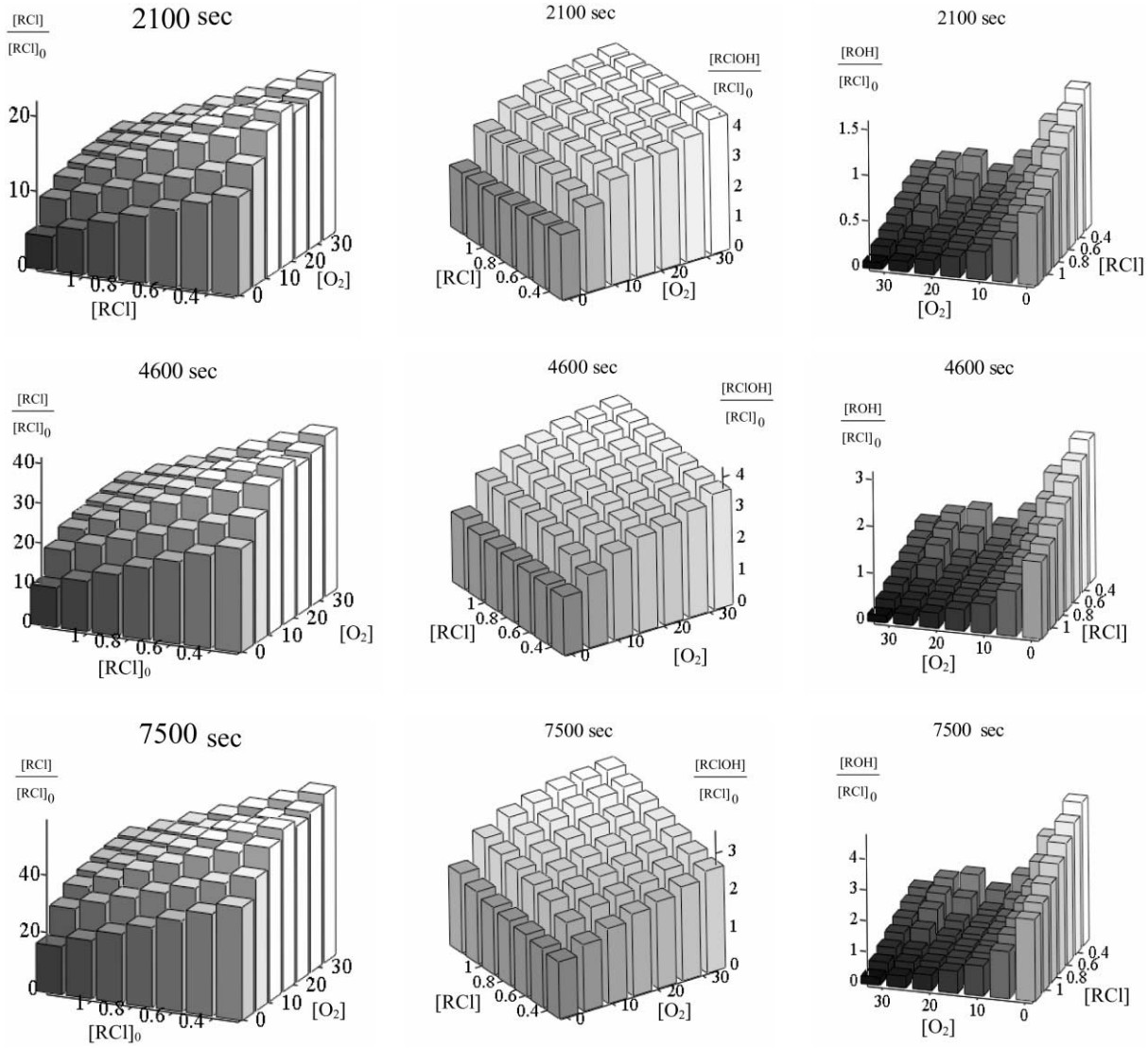

Fig. 8. Result of the kinetic model showing a 3D view of 3,4-dichlorophenol disappearance as a function of initial concentration and oxygen level at 2100, 4600 and 7600 s reaction times, respectively, to the left and yield of OH addition in the middle and Cl removal to the right.

The discrepancy between the theoretical prediction and the experiment can be attributed in part to a single value for K_{ads} for all the compounds and significant variations of catalyst plate activity in the various runs. However, considerable effort was put in to using well characterised plates that have minimised this spread in activity as far as possible.

The model predicts the rate of parent compound degradation should decrease with the parent compound concentration, yet, the dechlorination rate should behave oppositely.

Remarkably, all of these novel trends are seen experimentally. The model gives a reasonable overall prediction of the reaction state space spanned by the parent and intermediate compound concentration, dissolved oxygen concentration and time.

6. Summary and conclusion

It is argued here that a hydroxyl radical is ejected from the catalyst surface by photo-excitation onto a repulsive excited electronic state leading to a translationally hot OH($^2\pi$) radical. A detailed study of the kinetics of photo-oxidation of 3,4-dichlorophenol at various concentrations in oxygenated solutions on TiO_2 and TiO_2/SnO_2 catalyst plates, suggests that slowing down of electron–hole recombination is not the primary rate enhancing property of dissolved oxygen. In all cases, the active oxide is TiO_2. In the presence of molecular oxygen, simple hydroxyl addition to the dichlorophenol occurs. In the absence of an adsorbed oxygen molecule, electron transfer to the aromatic ring from a Ti^{3+} site causes partial dechlorination of the dichlorophenol. Subsequently,

hydroxyl radical addition to the aromatic ring may occur. Hence, we find that dissolved molecular oxygen has two important roles in the photo-oxidation of 3,4-dichlorophenol on the semiconducting TiO_2 surfaces. One of these is as a H-atom acceptor required in direct hydroxyl radical addition to the phenyl ring; while the other is as an electron transfer inhibitor when adsorbed at defective Ti^{3+} sites. A theoretical model of the kinetics is proposed. Significantly, monitoring of the intermediate species produced by these two routes shows that the relative yields can be inverted by changing the dissolved oxygen concentration which is significantly in accordance with the theoretical predictions.

Acknowledgements

Anna-Karin Axelsson thanks South Bank University for a Scholarship, and Drs. G. Lawless, H. Cox and Prof. Bryan Reuben for helpful discussion.

References

[1] W.H. Glaze, J.F. Kenneke, J.L. Ferry, Chlorinated byproducts from the TiO_2 mediated photodegradation of trichloroethylene and tetrachloroethylene in water, Environ. Sci. Technol. 27 (1) 1993.
[2] K. Nishida, S. Ohgaki, Photolysis of aromatic chemical compounds in aqueous TiO_2 suspension, Water Sci. Technol. 30 (9) (1994) 39–46.
[3] G.V. Buxton, C.L. Greenstock, P.W. Helman, A.B. Ross, Critical review of rate constants for reactions of hydrated electrons, hydrogen atoms and hydroxyl radicals (OH/O^-) in aqueous solution, J. Phys. Chem. Ref. Data 17 (2) (1988).
[4] M.J. Perkins, in: J.K. Kochi (Ed.), Free Radicals, Vol. 2, Wiley, New York, 1973, p. 231.
[5] L.J. Dunne, H. Guo, J.N. Murrell, The role of the B-X conical intersection in the photodissociation of water, Mol. Phys. 62 (2) (1987) 283–294.
[6] L.J. Dunne, Farad. Discus. Chem. Soc. 82 (1986) 190/191.
[7] C. Turchi, D.F. Ollis, Photocatalytic degradation of organic water contaminants: mechanisms involving hydroxyl radical attack, J. Catal. 122 (1990) 178–191.
[8] A. Mills, S. Le Hunte, An overview of semiconductor photocatalysis, J. Photochem. A: Chem. 108 (1997) 1–35.
[9] M.R. Hoffman, T.M. Scot, C. Wonyong, D.W. Bahneman, Environmental application of semiconductor photocatlysis, Chem. Rev. 95 (1995) 69–96.
[10] M.A. Fox, M.T. Dulay, Heterogeneous photocatalysis, Chem. Rev. 93 (1) (1993) 341–354.
[11] P.V. Kamat, Photochemistry on nonreactive and reactive (semiconductor) surfaces, Chem. Rev. 93 (1993) 267–300.
[12] A. Mills, J. Wang, Photomineralisation of 4-chlorophenol sensitised by TiO_2 thin films, J. Photochem. Photobiol. A: Chem. 118 (1998) 53–63.
[13] N. Serpone, I. Texier, A.V. Emiline, P. Pichat, H. Hidaka, J. Zhao, Post-irradiation effect and reductive dechlorination of chlorophenols at oxygen-free TiO_2/water interfaces in the presence of prominent hole scavengers (2000), J. Photochem. Photobiol. A: Chem. 136 (2000) 145–155.
[14] W.Z. Tang, C.P. Huang, Effect of chlorine content of chlorinated phenols on their oxidation kinetics by Fenton's reagent, Chemosphere 33 (8) (1996) 1621–1635.
[15] L. Rideh, A. Wehrer, D. Ronze, A. Zoulalian, Modelling of the kinetic of 2-chlorophenol catalytic photooxidation, Catal. Today 48 (1999) 357–362.
[16] A.L. Linsbergler, G. Lu, J.T. Yates Jr., Chem. Rev. 95, 1995.
[17] A. Vittadini, F.P. Selloni Rotzinger, M. Gratzel, Structure and Energetics of Water Adsorbed at TiO_2 Anatase (1 0 1) and (0 1) Surface, Phys. Rev. Lett. 81 (14) (1998).
[18] C.S. Turchi, D.F. Ollis, An example of mass-transfer limitations with an immobilised catalyst, J. Phys. Chem. 92 (1988) 6852–6853.
[19] J. Goniakowski, M.J. Gillan, The adsorption of H_2O on TiO_2 and SnO_2 (1 1 0) studied by first principles calculations, Surf. Sci. 350 (1996) 145–158.
[20] N.F. Mott, E.A. Davies, Electronic Processes in Non-crystalline Materials, Oxford University Press, Oxford, 1971.
[21] S.A. Roulston, L.J. Dunne, A.D. Clark, M.F. Chaplin, Philos. Mag. B 62 (1990) 243.
[22] D.R. Lide (Ed.), CRC Handbook of Chemistry and Physics, 76th Edition, CRC Press, New York.
[23] L.J. Dunnel, J.P. Braga, J.P. Murrell, A comparison of classical and quantal transition probabilities for non-adiabatic atom–atom collision, Chem. Phys. Lett. 120 (1985) 147–150.
[24] R.D. Levine, R.B. Bernstein, Molecular Reaction Dynamics, Clarendon Press, Oxford, 1974, p. 87.